Investigation of photoexcitations of conjugated polymer/fullerene composites embedded in conventional polymers

C. J. Brabec,[a] V. Dyakonov, and N. S. Sariciftci
Physical Chemistry, Johannes Kepler University Linz, Austria

W. Graupner and G. Leising
Institute for Solid State Physik, Technical University Graz, Austria

J. C. Hummelen
Material Science Center, University of Groningen, The Netherlands

(Received 16 March 1998; accepted 9 April 1998)

A promising approach to improve the processability of semiconducting polymers is their incorporation into host matrices formed by conventional polymers such as polyethylene (PE) or polystyrene (PS). We have characterized the linear optical properties of several guest–host systems by absorption and luminescence measurements and probed the excited states by photoinduced absorption measurements (PIA) and light induced electron spin resonance (LESR). The interesting photophysics of conjugated polymer/fullerene donor–acceptor system, showing an ultrafast photoinduced electron transfer and a metastable charge separation in the pristine state, has been investigated in such composites where the photoactive components are further embedded into a conventional polymer matrix. The composition of the blend and the relative concentration of the components are found to strongly influence the photoinduced interaction between the conjugated polymer and the fullerenes (C_{60} and functionalized fullerenes). Photoinduced electron transfer between a soluble polyphenylenevinylene (PPV) derivative and C_{60} is observed in a system with PS as host when the concentration of the both electroactive components is 33%. In diluted composites with PS as matrix we find strong luminescence quenching of the PPV derivative but no electron transfer upon adding C_{60}. Dominant photoexcitations in these PS systems are triplet states as follows from intensity dependencies and lifetime measurements. In diluted systems with PE as matrix neither charge transfer nor luminescence quenching has been observed. © *1998 American Institute of Physics.* [S0021-9606(98)51827-2]

I. INTRODUCTION

The utilization of the strong photoluminescence of conjugated polymers for light emitting devices resulted in emphasized research in this class of materials that combines the electronic and optical properties of semiconductors and metals with the attractive mechanical properties as well as processing properties of polymers.[1–4] But also polymer systems exhibiting photoinduced electron and/or energy transfer find more and more attraction in the scientific community due to the possibility to utilize these systems for solar energy conversion.[5] The characterization of C_{60} as an electron acceptor capable of accepting as many as six electrons[6] candidates it as the acceptor in blends with conjugated polymers as good photoexcited electron donors. A wide class of these conjugated polymers and oligomers show a photoinduced electron transfer from the excited state of the conjugated polymer onto the buckminsterfullerene, C_{60}.[7,8] The stabilization of the charge separated state in the conjugated polymer is assumed to result from the stability and delocalization of the positive polaron on the conjugated polymer backbone. Additionally, the excellent acceptor properties of C_{60} due to structural relaxation of the fullerene following the photoexcitation is assumed to help forming long living charges in these composites. The forward electron transfer to C_{60} occurs faster than in 1 ps thereby strongly quenching the photoluminescence as well as triplet exciton formation of the conjugated polymer.[9] This implies, that this process is efficiently competing with the dipole-allowed radiative emission as well as other nonradiative channels. However, the successful and efficient charge separation is influenced by a number of limiting factors. Generally, the ionization potential of the excited state of the donor (I_{D*}), the electron affinity of the C_{60} ($A_{C_{60}}$) and the Coulomb attraction of the separated radicals (U_C) including the polarization effects should match the following inequality:

$$I_D - A_{C_{60}} - U_C < 0. \tag{1}$$

Studies by Janssen *et al.*[10] pointed out, that Eq. (1) is a necessary but not sufficient condition. Some other factors may inhibit the charge transfer such as a potential barrier preventing the separation of the photoexcited electron–hole pair or the morphology of the blend preventing the overlap of the donor and acceptor excited state wave functions due to too large intermolecular spacings.

[a]Corresponding author: Christoph Josef Brabec, Institute of Chemistry/Physical Chemistry, Johannes Kepler University Linz, Austria, Altenbergerstr. 69, A-4040 Linz, Austria/Europe. Electronic mail: christoph.brabec@jk.uni-linz.ac.at

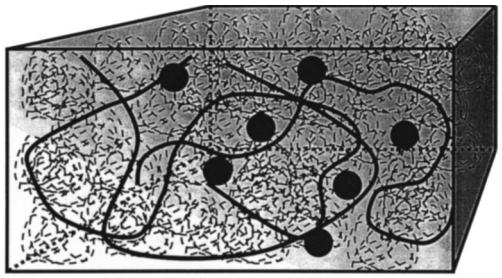

FIG. 1. Schematic draw of the conjugated polymer (—full line)/fullerene [full circle (●)] embedded in a conventional polymer host matrix [dashed line (--)].

Photoinduced charge transfer phenomena described by Marcus[11,12] showed, that the rate of the forward as well as the back electron transfer depends on the polarity of the surrounding matrix. Recently, increasing emphasis in research of conjugated polymers is placed on the engineering and processing of the conjugated polymer in blends and composites with conventional polymers.[13–16] In these blends conventional polymers with excellent optical and mechanical properties like polymetamethylacrylate (PMMA), polystyrene (PS), polyethylene (PE), polyvinylchloride (PVC), or polycarbonate (PC) can be used as host matrices. The guest–host approach is a sound method to improve the sample quality to enable the investigation of one dimensional systems for the following reasons:

(1) In free standing films of these blends, the highly diluted conjugated polymer, which may be compared to solid solutions, shows less interchain interaction compared to pure films.
(2) Macroscopic ordering and orientation of the conjugated polymer can be performed by mechanical uniaxial stretching of the host polymer.
(3) In polymer blends the conjugated polymers are encapsulated in a highly stable host polymer, which protects the conjugated polymer against environmental influences.

In this work we report results of quasi-steady-state photoexcitation spectroscopy on conjugated polymer/fullerene composites blended in conventional host polymers. A schematic picture of the morphology of such composites is given in Fig. 1. The spectroscopical methods used are photoinduced absorption spectroscopy (PIA) in the UV/VIS and near infrared as well as light induced electron spin resonance (LESR). The conjugated polymer is in all cases poly[2-methoxy, 5-(2′-*ethyl-hexyloxy*)-*p*-phenylene vinylene], hereafter referred to as (MEH-PPV). Three different fullerenes have been used as electron acceptors, the nonsubstituted C_{60} and two solubilized fullerenes, $PC_{61}BCR$ ([5,6]-Phenyl-C_{61}-Butyric acid CholesteRyl) and $PC_{61}BM$(Phenyl)C_{61}B(utoxy)M(ethoxy).[17] The structure of the compounds is shown in Fig. 2. The conventional host polymers are either PE or PS. In each case we have studied the conjugated polymer and the fullerene alone in the matrix to investigate the influence of the host on the electrooptical properties of the guest components.

We show that the choice of the host polymer and the concentration of the embedded components strongly influence the dominant photoexcitation. Surprisingly, in diluted PS systems we observe luminescence quenching but no photoinduced electron transfer upon adding C_{60}.

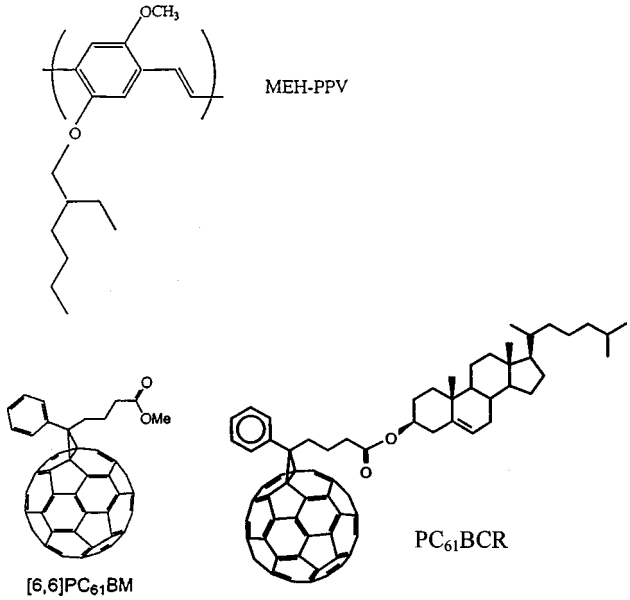

FIG. 2. Chemical structure of MEH-PPV, $PC_{61}BCR$, and $PC_{61}BM$.

II. EXPERIMENT

MEH-PPV has been provided by the UNIAX Corporation, Santa Barbara. The synthesis is described in the literature.[18] Films of MEH-PPV in PE (1 wt % MEH-PPV in UHMW-PE) have been prepared by gel processing as described elsewhere.[19,20] Highly oriented films have been produced by mechanical stretching in a stress–strain rheometer at 110–120 °C alternatively to a route, where films are stretched by hand over a hot pin. The stretch ratio is approximately 10. In the same way the PE/MEH-PPV/fullerene films have been produced. As preliminary investigations showed, PE and C_{60} have a very low miscibility. Therefore, we use a special soluble C_{60} derivative. The weight ratio of $PC_{61}BCR$ to MEH-PPV is 2:1.

For the PS blends we have used a Hoechst PS N168. The pure reference systems (either MEH-PPV or C_{60} in PS) have been prepared by mixing MEH-PPV or C_{60} (2 wt %) with PS in toluene. After 24 h of mixing free standing films have been produced by drop casting on clean microscope slides and drying under nitrogen flow. The PS/MEH-PPV/C_{60} films have been prepared in various concentrations. For the absorption, luminescence and PIA measurements in the UV/VIS following composites have been investigated: PS:MEH-PPV:C_{60}=100:2:2, 100:2:6, 100:2:10. These, with respect to the electroactive components *diluted samples* are subsequently referred to as *low, intermediate and high* C_{60} *composite*.

Composites with equal weight ratios (1:1:1) of PS:MEH-PPV:C_{60} have been investigated by LESR measurements. Photoinduced FTIR and again LESR measurements have also been performed on a composite with equal

weight ratios of PS, MEH-PPV, and a highly soluble fullerene, the $PC_{61}BM$. Samples from these concentrations, hereafter referred to as *concentrated samples*, have been prepared from appr. 1 wt % solutions in *o*-dichlorobenzene (ODCB) (for the C_{60} composite) or xylene (for the $PC_{61}BM$ sample).

The absorption spectra are measured on a Hitachi UV/VIS spectrometer. For taking luminescence spectra samples have been placed in an evacuated liquid nitrogen bath cryostat. The chopped 488 nm beam of a argon laser serves as pump source. Luminescence is then measured with a monochromator and a Si photodiode by a lock-in amplifier. The PIA measurements are made in a two beam technique. A chopped argon–ion laser beam is used to generate photoexcited states in the sample, which are detected by analyzing the change in transmission of a white light tungsten halogen lamp. Transmission is measured using a lock-in amplifier with a monochromator and a Si detector. In all cases the free standing films have been placed between two sapphire substrates and mounted to a cold finger of the liquid nitrogen cryostat.

LESR measurements are performed on Bruker EMX spectrometer with a 200 MHz broadband bridge with an Ar^+ laser (488 nm, 70 mW) as a pump. Samples were placed in a rectangular high Q cavity with a 50% grid for illumination. Samples for LESR investigations have been prepared in 3 mm Wilmad EPR tubes from solutions with concentrations as described above. After pouring approximately 0.2 ml of polymer solution into the ESR tube the solvent was evaporated in inert atmosphere. After complete drying of the films on the inner side of the tubes samples were covered with the thin film. The tubes are evacuated up to 10^{-5} Torr and sealed.

Infrared activated vibrational (IRAV) spectra are studied on a Bruker IFS 66S spectrometer with a liquid nitrogen cooled MCT detector. Samples are prepared by drop casting from polymer solution on pressed KBr pellets. After evaporation of the solvent in a nitrogen flow box, the pellets are mounted on the cold finger of an evacuated liquid nitrogen bath cryostat with ZnSe windows. The vacuum for all measurements was better than 10^{-6} Torr. The samples are illuminated through a 90° geometry quartz window of the cryostat with 20 mW/cm^2 of 488 nm line of an Ar^+ laser. Spectra are recorded by 200 accumulations of 10 dark and 10 illuminated cycles, to increase the signal to noise ratio.

III. RESULTS

Before the presentation of the experimental results on the MEH-PPV/fullerene guest in the PE or PS host matrix, we briefly summarize the spectroscopic results of pure MEH-PPV/C_{60} blends, where photoinduced electron transfer reactions are well studied.[4] A dominant peak in PIA measurements at 1.34 eV in pure MEH-PPV films is attributed to triplet–triplet absorption. In addition, several new features are observed in composites with C_{60}: a peak around 1.4 eV, a distinct shoulder at 1.18 eV, and a plateau from 1.5 to 2 eV. Absorption detected magnetic resonance measurements[21] show, that the peak around 1.34 eV in pure MEH-PPV and MEH-PPV/C_{60} have different natures, being associated with triplet states in pristine MEH-PPV films and to spin-$\frac{1}{2}$ polarons in the mixed films.[10] In addition to the changes in the PIA spectrum, the photoluminescence of MEH-PPV is strongly quenched upon addition of C_{60}. Photoinduced electron transfer is manifested by appearance of two LESR signals with *g* factors slightly smaller and larger than two.[7] These lines are attributed to the C_{60}^- radical and the positive polaron on the polymer, respectively.

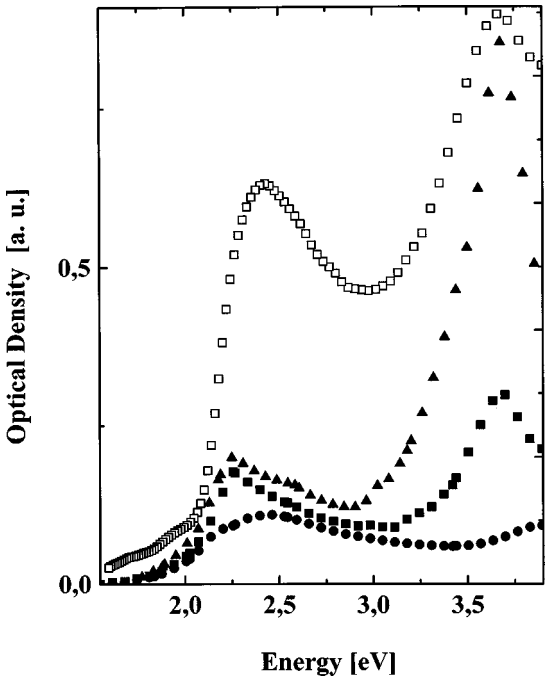

FIG. 3. Absorption data of PE/MEH-PPV/$PC_{61}BCR$ and PS/MEH-PPV composites with different concentrations of C_{60} at room temperature. Spectra have been recorded from free standing films. The notation of the curves is: empty squares (□) PE/MEH-PPV $PC_{61}BCR$, full circles (●) PS/MEH-PPV, full squares (■) PS/MEH-PPV/low C_{60} and full triangles (▲) PS/MEH-PPV/high C_{60}.

A. PE composites

Figure 3 shows the absorption spectra of the composites. The onset of absorption for MEH-PPV is observed at 2.1 eV and the maximum of absorption is at 2.45 eV. These values are comparable to the literature.[22] Compared to the PS samples, in samples with PE as a host the absorption maximum of MEH-PPV is slightly blueshifted. A second peak around 3.7 eV is attributed to fullerene absorption. A further absorption peak from MEH-PPV cannot be seen in these absorption spectra, as the high energy region of the spectra are dominated by the strong fullerene absorption. The relative intensity of the peak heights in the absorption spectra allows one to estimate the ratio of fullerene content in the single samples. All absorption data shown here are taken on free standing films produced by drop casting from solution, yielding films with different thicknesses.

Figure 4 shows the luminescence spectra of the pristine PE/MEH-PPV gel and of a composite with PE/MEH-PPV/$PC_{61}BCR$, the latter has been stretched by approximately ten times. Utilizing the enhanced solubility of $PC_{61}BCR$ compared to C_{60} it was possible to make gels with higher optical

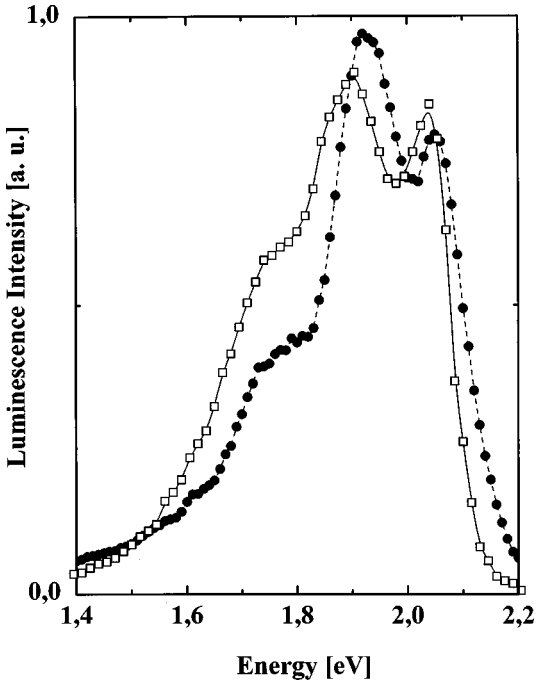

FIG. 4. Luminescence data of PE/MEH-PPV composites with [hollow squares (□)] and without [full circles (●)] $PC_{61}BCR$ at 80 K and 10^{-5} Torr. The weight ratio between MEH-PPV and $PC_{61}BCR$ is 1:2. For the oriented sample the 488 nm pump beam is parallel to the stretch direction.

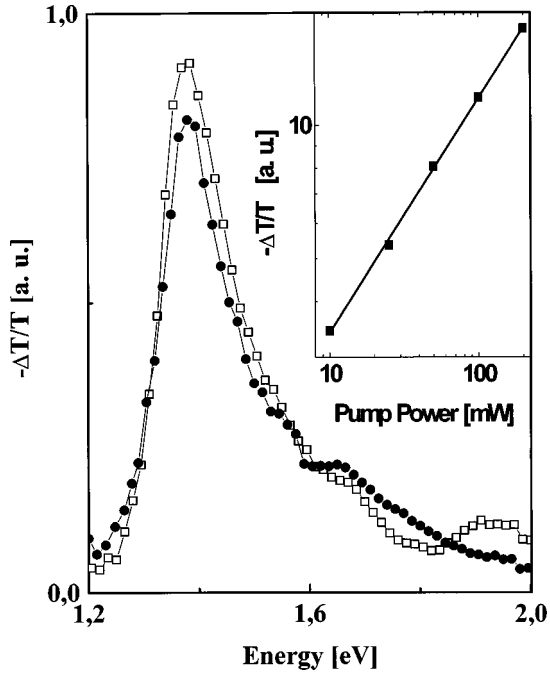

FIG. 5. $-\Delta T/T$ of PE/MEH-PPV composites with [hollow squares (□)] and without [full circles (●)] $PC_{61}BCR$ at 80 K and 10^{-5} Torr. The weight ratio between MEH-PPV and $PC_{61}BCR$ is 1:2. For the oriented sample the 488 nm pump beam is parallel to the stretch direction, the probe beam is unpolarized. The inset shows the scaling behavior of the 1.41 eV peak on the pump intensity. Nonlinear fitting with a power law $y=a*x^{\alpha}$ gives a scaling exponent $\alpha=0{,}53$.

quality. Measurement data are normalized according to the different film thicknesses calculated from the absorption spectrum. One can see clearly, that addition of up to 2 wt % of fullerenes to the PE/MEH-PPV gel does not quench the luminescence of MEH-PPV. Both spectra show similar vibronic structures. The redshift of 0,05 eV of the sample with $PC_{61}BCR$ compared to the pure sample may be explained by the higher orientation due to the stretching and is in accordance with the literature.[16]

The PIA spectra of the both samples are shown in Fig. 5. Spectra have been corrected for their different optical densities (OD) via Eq. (2)

$$-\frac{\Delta T}{T_{\text{corrected}}}=\frac{\dfrac{-\Delta T}{T}}{1-10^{-\text{OD(488 nm)}}}. \tag{2}$$

Pumping with higher intensities of up to 200 mW does not result in spectral changes. The dominant feature in both spectra, with and without $PC_{61}BCR$ is a PIA peak at 1.37 eV. This peak with a low energy onset at 1.2 eV is rather broad and reveals a highly asymmetric shape to the high energy side. Intensity dependence measurements of the sample with $PC_{61}BCR$, shown in the inset of Fig. 5, can be fitted best with a scaling exponent of $\alpha=0.53$, which indicates a relaxation mechanism dominated by bimolecular behavior, similar to unblended MEH-PPV films.[23] In spite of the bimolecular nature, the peak has been generally accepted to arise from triplet–triplet absorption.[9,10] Frequency dependent measurements have been performed by increasing the chopping speed and yield a lifetime of the 1.37 eV peak 0.7 ms. Increasing the weight ratio of fullerenes relative to MEH-PPV (4:1 instead of 2:1) further deteriorates the film quality and results in inhomogeneous gels. Even the highly soluble $PC_{61}BCR$ tends to phase segregate from PE, so that increasing the amount of fullerenes only leads to enhanced clustering.

B. Diluted PS composites

1. Absorption and luminescence data

Absorption data of PS/MEH-PPV/C_{60} composites with various concentrations have already been presented in Fig. 3. One can see how the C_{60} absorption peak grows with increasing amount of fullerenes, indicating that C_{60} shows less tendency to form clusters in PS compared to PE. However, comparing the fullerene weight percentage of the low and the high C_{60} sample in the solution (factor of 5) to the ratio of the absorption peaks in the films (appr. factor of 3), one can see that not all of the fullerene molecules mixed into the solution contribute to the absorption in the film. The height of the fullerene absorption peak shows saturation upon increasing the amount of C_{60}, indicating that PS and C_{60} are no longer fully miscible at higher fullerene concentrations. The onset of MEH-PPV absorption is at 2.1 eV. The MEH-PPV maximium of the film without fullerene is at 2.45 eV, while the films with low and high C_{60} concentration have their maximum at 2.25 eV. Although the films differ only in the fullerene concentration, their optical density for the MEH-PPV absorption is different. Free standing films from compounds with C_{60} are thicker than comparable compounds without C_{60}.

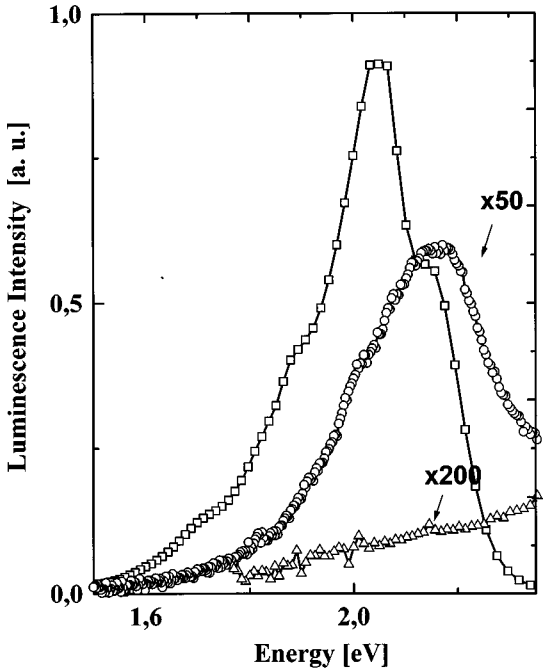

FIG. 6. Luminescence measurements of PS/MEH-PPV samples with different concentrations of C_{60} at 80 K and 10^{-5} Torr. The notation of the curves is: hollow squares (□) PS/MEH-PPV, hollow circles (○) PS/MEH-PPV/low C_{60} (scaled 50 times) and hollow triangles (△) PS/MEH-PPV/high C_{60} (scaled 200 times).

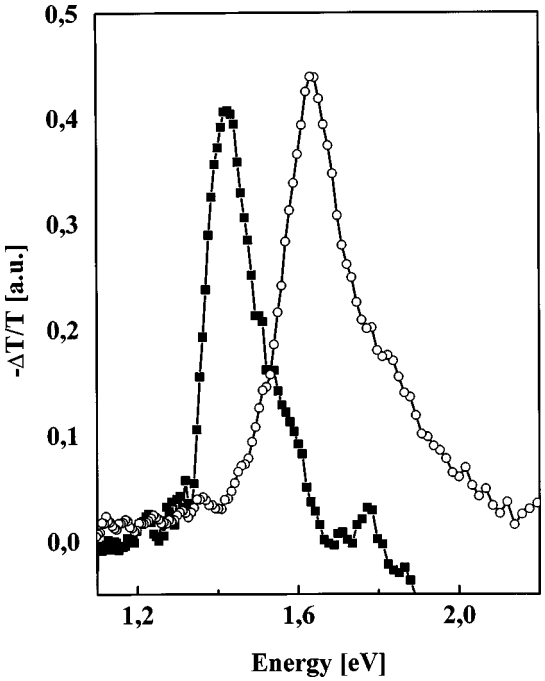

FIG. 7. $-\Delta T/T$ for PS/MEH-PPV [full squares (■)] and PS/C_{60} [hollow circles (○)] composite at 80 K and 10^{-5} Torr. The energetic position of the PS/MEH-PPV peak is at 1.41 eV, the peak of the PS/C_{60} system is at 1.63 eV.

The luminescence spectra of free standing PS/MEH-PPV/C_{60} films are shown in Fig. 6. The intensities have been corrected for the different amount of absorbed light due to different film thickness by comparison of the MEH-PPV absorption peaks. The figure shows the luminescence for the pure PS/MEH-PPV system as well as for the low and high C_{60} sample. The most important finding is the quenching of luminescence upon addition of C_{60}. In the low C_{60} sample, containing approximately equal weight amount of C_{60} and MEH-PPV, luminescence is quenched by a factor of 80, while in the high C_{60} composite luminescence is quenched nearly completely. Luminescence spectrum of the PS/MEH-PPV composite has a main peak at 2.05 eV and two weak shoulders, one very weak at 1.9 eV and one around 2.15 eV. Alternation in the vibronic fine structure is well known for blends of conjugated polymers and conventional polymers.[24–26] The luminescence maxima of the low C_{60} component at 2.18 eV is blueshifted by 0.12 eV compared to the pure PS/MEH-PPV component.

2. Quasi-steady-state photoinduced absorption

The photoexcited states of the diluted PS composites and their dependencies on the lifetime as well as on pump intensity are investigated by PIA measurements and presented in Figs. 7–10. All spectra are corrected due to the different absorption of the films studied according to Eq. (2). Figure 7 shows $-\Delta T/T$ for the two reference systems PS/MEH-PPV as well as PS/C_{60}. The dominant photoinduced feature of the PS/MEH-PPV sample is a peak at 1.41 eV. This peak has a sharp low energy onset at 1.35 eV and decays asymmetrically at the high energy side. The photoinduced spectrum, after correction for luminescence, changes the sign around 1.9 eV indicating phonon assisted bleaching. Intensity dependence measurements, shown in Fig. 8(a), can be best fitted with a scaling exponent of $\alpha = 0.56$. This implies a decay behavior dominated by bimolecular relaxation, confirmed by saturation behavior for pump powers higher than 300 mW. Frequency dependence studies fitted by a bimolecular decay model yield a relaxation time of 0.6 ms [Fig. 8(b)]. Although the bimolecular relaxation behavior, it is generally accepted to identify this peak at 1.41 eV as the MEH-PPV triplet peak.[22] The PIA PS/C_{60} spectrum (see Fig. 7) again is dominated by one single peak, located at 1.63 eV. Figures. 8(a) and 8(b) show frequency and intensity dependencies of this peak. The scaling exponent of the pump intensity is calculated with $\alpha = 0.97$, which gives rise to the assumption of a monomolecular dominated decay behavior. The relaxation time fitted by a monomolecular decay model is found to be 1.1 ms. We therefore identify the 1.63 eV peak as the C_{60} triplet peak.[27]

Figure 9 shows the results for PS/MEH-PPV/C_{60} composites with three different C_{60} concentrations. PIA measurements of the low C_{60} sample plotted in Fig. 9 show a broad, structureless peak between 1.4 and 1.7 eV with a maximum around 1.51 eV. When the concentration of C_{60} in the sample is increased (intermediate C_{60} sample), $-\Delta T/T$ changes its shape. A new peak arises at 1.63 eV while the old peak at 1.51 eV of the low C_{60} sample is quenched and remains as a weak shoulder. Further increasing of the C_{60} concentration (high C_{60} sample) contributes directly to the 1.63 eV peak. Figure 10 shows the intensity dependence of low C_{60} peak at five different energy positions. The scaling exponents, determined by fitting of the curves range between $\alpha = 0.5$ and α

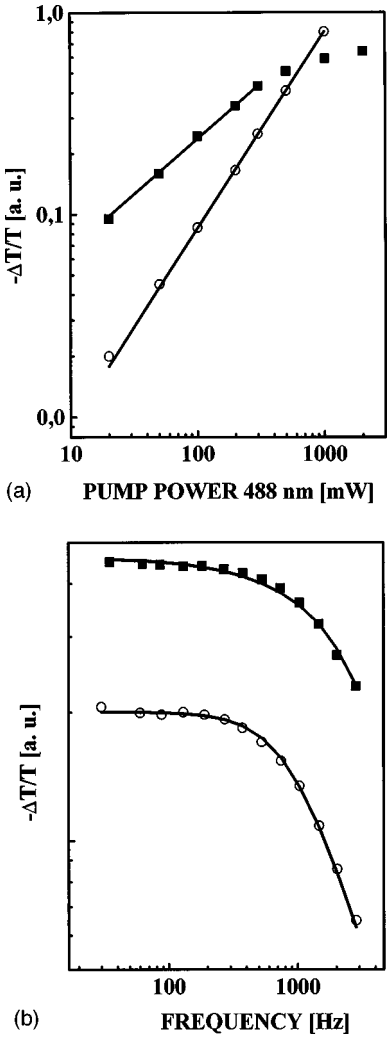

FIG. 8. Intensity (a) and frequency (b) dependence of the 1.41 eV MEH-PPV peak of the PS/MEH-PPV system [full squares (■)] and the 1.63 eV C_{60} peak of the PS/C_{60} system [hollow circles (○)]. Nonlinear fitting of the intensity dependencies with a power law $y=a^*x^{\alpha}$ gives a scaling exponent $\alpha=0{,}56$ for the MEH-PPV peak and $\alpha=0.97$ for the C_{60} peak. Fitting of the MEH-PPV peak with a bimolecular decay model yields a relaxation time of 0.6 ms while a fit with a monomolecular model for the C_{60} peak gives a relaxation time of 1.1 ms.

$=0.63$. This low scaling exponent implies a bimolecular decay mechanism. From frequency dependence measurements we estimate the relaxation time around 1 ms.

Figure 11 shows the PIA spectrum of the composite with the intermediate fullerene concentration, once pumped with 488 nm and once pumped in the UV with 354 nm. At a pump energy of 488 nm two spectral features can be seen, one peak at 1.63 eV and a low energy shoulder for which deconvolution of this spectrum delivers 1.41 eV. Upon pumping with 354 nm only the peak at 1.63 eV remains. In Fig. 11 the relative intensities of the PIA bands for different excitations appear to be different. However, correction of $-\Delta T/T$ according to Eq. (2) for the different absorption at the different pump energies yields no enhancement of the triplet–triplet PIA absorptions in this figure.

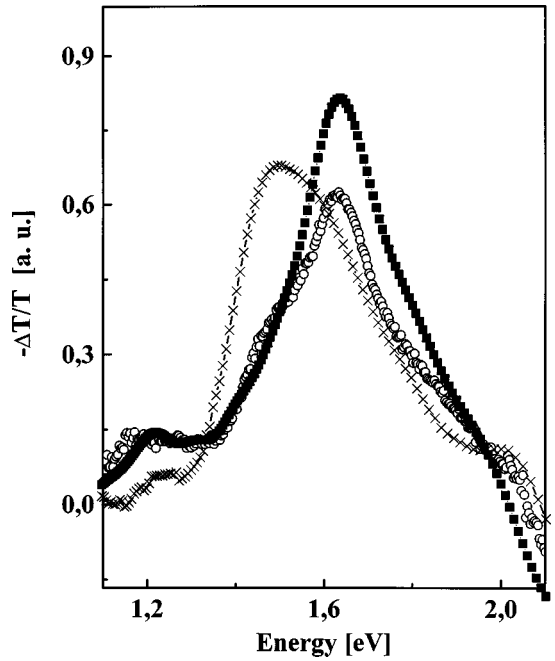

FIG. 9. $-\Delta T/T$ for PS/MEH-PPV samples with low [crosses (x)], intermediate [hollow circles (○)] and high C_{60} [full squares (■)] concentration at 80 K and 10^{-5} Torr. The energetic position of the peaks are 1.51 eV for the low concentrated system and 1.63 eV for the intermediate and high concentrated system.

C. Concentrated PS composites

1. LESR measurements

To exclude dark background signals from long living radicals and from permanent radicals due to sample impuri-

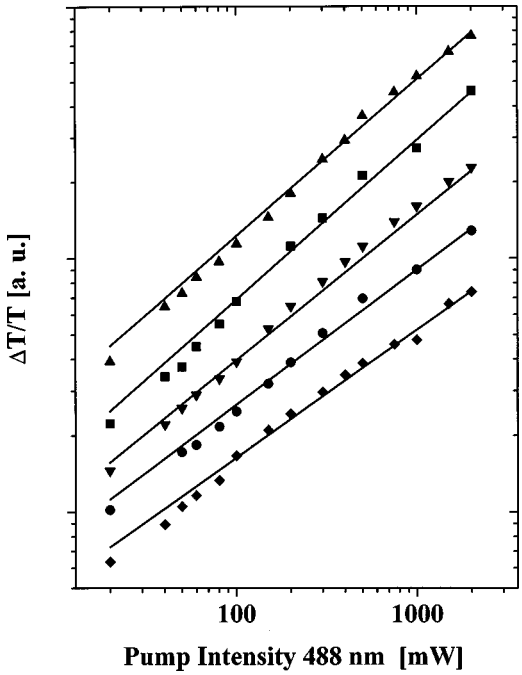

FIG. 10. Intensity dependence of the low C_{60} sample peak at five different positions from 1.4–1.7 eV. Lines are nonlinear fits with a power law $y=a^*x^{\alpha}$. The following data have been calculated: 1.4 eV [full karo (◆)], $\alpha=0.50$, 1.47 eV [full circles (●)], $\alpha=0.54$, 1.5 eV [full down triangles (▼)], $\alpha=0.57$, 1.61 eV [full squares (■)], $\alpha=0.63$, 1.69 eV [full up triangles (▲)], $\alpha=0.62$

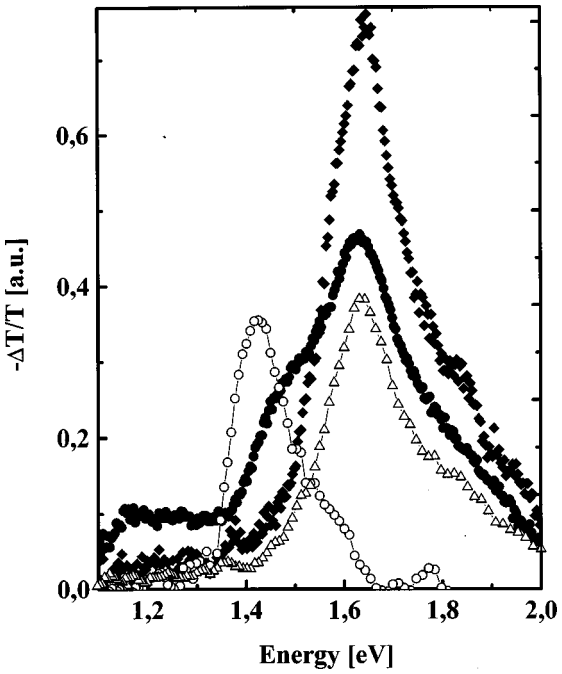

FIG. 11. $-\Delta T/T$ for PS/MEH-PPV samples with intermediate C_{60} pumped at 488 nm [full circles (●)] and at 354 nm [full karo (♦)] at 80 K and 10^{-5} Torr. For better comparison the two reference systems, PS/MEH-PPV [hollow circles (○)] and PS/C_{60} [hollow triangles (△)] are included.

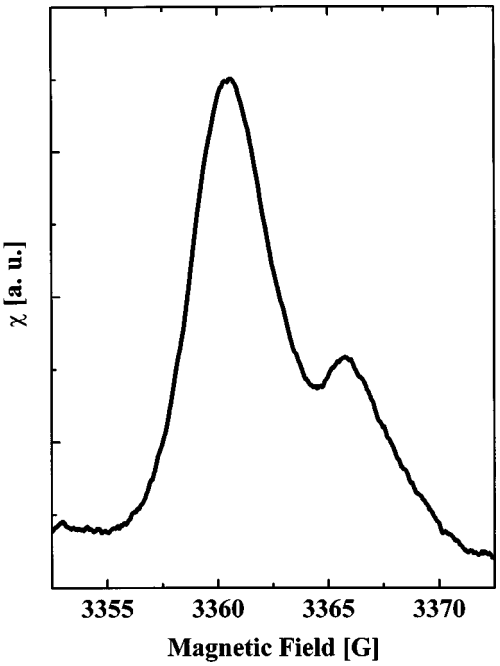

FIG. 13. Integral of LESR spectrum [full line (−)] of the concentrated PS/MEH-PPV/C_{60} compound presented in Fig. 12. Evaluation of the signal yields two peaks, one at low magnetic fields with a g value of $g=2.0023$ and one at higher fields with a g value of $g=1.9997$. Signals are interpreted as MEH-PPV$^+$ polaron and C_{60}^- anion, respectively.

ties, LESR measurements presented here have been performed in the following way. Samples have been cooled down to working temperature carefully avoiding any illumination. ESR measurement under this condition is referred to as dark signal. To separate different contributions to ESR signals we subsequently performed two ESR measurements, ''light on'' and ''light off.'' It should be mentioned, that switching off the light does not result in the reappearance of the dark ESR signal, rather a persistent ESR signal remains. Therefore, all spectra are corrected by subtraction of the light off spectrum from the light on spectrum. Only the difference spectrum between them is interpreted as the prompt LESR signal.

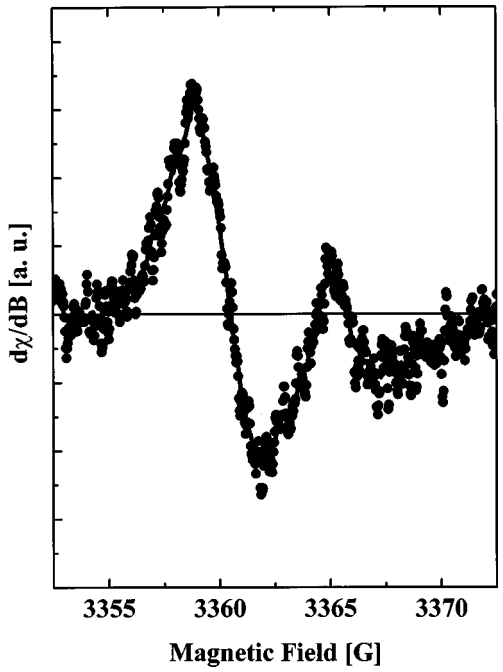

FIG. 12. LESR spectrum [full circles (●)] of the concentrated PS/MEH-PPV/C_{60} compound with equal weight ratios. The line represents data after smoothing by a Savitzky Golay filter. LESR spectrum is recorded at 100 K and 10^{-4} Torr as the difference between the illuminated signal and the signal after switching off the light. Illumination is provided through a 50% grid by 70 mW of the 488 nm line of an Ar^+ laser. Micorwave power is 2 mW. Prior to illumination samples are heated up to room temperature to relax long living radicals and cooled down to 100 K.

Dark ESR spectrum for the sample PS/MEH-PPV/C_{60} with equal weight ratios, recorded at 100 K, does not show radical features. Under illumination two detailed features can be seen: one signal at $g=1.9997$ and another signal at $g=2.0023$. After subtraction of the light off spectrum from the illuminated one two signals at $g=1.9997$ and $g=2.0023$ with $\Delta H_{pp}=1.7$ G (where ΔH_{pp} is the peak to peak linewidth) and $\Delta H_{pp}=3.5$ G, respectively, are seen and presented in Fig. 12. The presence of two lines is more clearly seen after integration of the LESR spectrum (Fig. 13). The integrated LESR spectrum shows two peaks with different areas. The area under the peaks corresponds to the number of photogenerated paramagnetic radicals. However, different radical species may show different saturation behavior. Therefore, comparison of the number of photogenerated radicals can only be done, when both ESR signals are not saturated. Saturation behavior of LESR signals for charge transfer systems is discussed more detailed by Dyakonov *et al.*[28]

Figure 14 shows the LESR spectrum for a composite of the same concentration as described above, only C_{60} has been exchanged by the better soluble $PC_{61}BM$. Again, the first dark measurement after cooling the evacuated tube from

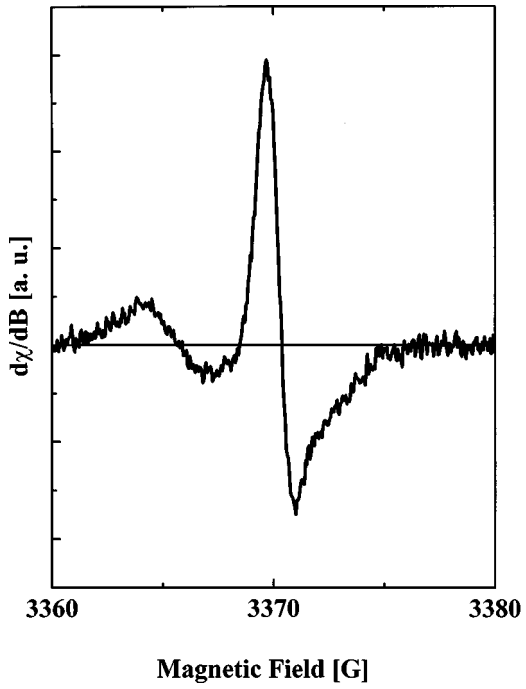

FIG. 14. LESR spectrum [full line (−)] of the concentrated PS/MEH-PPV/$PC_{61}BM$ compound with equal weight ratios. LESR spectrum is recorded under identical conditions as the PS/MEH-PPV/C_{60} sample as the difference between the illuminated signal and the signal after switching off the light. Microwave power is 0.2 mW.

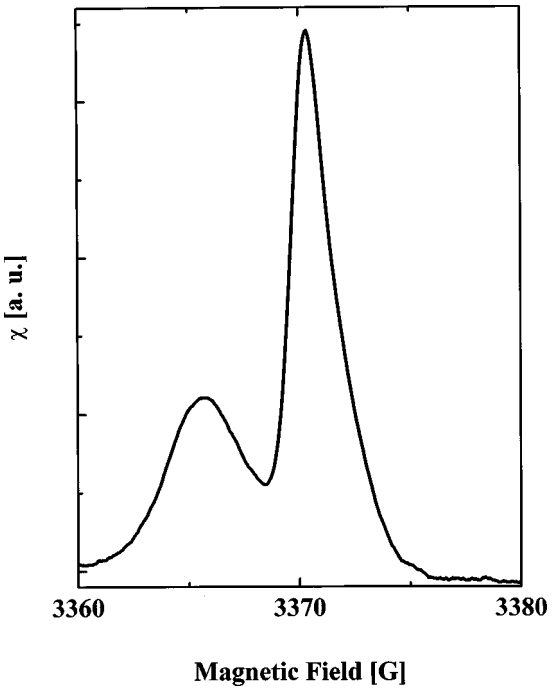

FIG. 15. Integral of LESR spectrum [full line (−)] of the concentrated PS/MEH-PPV/$PC_{61}BM$ compound presented in Fig. 14. Evaluation of the signal yields two peaks at identical g values as for the PS/MEH-PPV/C_{60} sample at $g=2.0023$ and at $g=1.9997$. Therefore peaks are interpreted as MEH-PPV^{+} polaron and $PC_{61}BM^{-}$ anion, respectively.

room temperature to 100 K does not reveal radical features. Spectrum consists of two photogenerated signals, the high field signal at $g=1.9997$ with a linewidth $\Delta H_{pp}=1.4$ G and the low field signal at $g=2.0023$ with a linewidth $\Delta H_{pp}=3.5$ G. LESR signals are more intense compared to the sample with C_{60} instead of the $PC_{61}BM$. Saturation analysis confirms the finding that the two different peaks belong to different species of light induced radicals. Integration of the LESR spectrum (Fig. 15) shows two peaks. The second integral of the LESR curve shows that the two different species of radicals are photogenerated with equal amount.

Reversibility of the photoinduced generation of radicals is demonstrated by the possibility of annealing at temperatures higher than 200 K. Subsequent LESR measurement cycles of heating to 290 K, cooling down to 100 K, illumination with light, switching light off and heating up again yield identical results.

2. Photoinduced IRAV measurements

The IRAV spectrum of the PS/MEH-PPV/$PC_{61}BM$ with equal weight ratios is shown in Fig. 16(a) together with the spectrum for a composite without $PC_{61}BM$ (PS/MEH-PPV with equal weight ratios). Figure 16(b) zooms out the low energy part of the spectrum. The spectrum of the composite with $PC_{61}BM$ clearly reveals a subgap electronic absorption band at 0.36 eV and a strong enhancement (by more than an order of magnitude) of the infrared active vibrational modes compared to the spectrum of the composite without fullerene. The value for the subgap electronic absorption band has been reported earlier for pristine MEH-PPV.[29] Additional strong IRAV bands are seen at 0.18 and at 0.13 eV.

In order to check the influence of the host matrix PS on the photoexcited states of the MEH-PPV/$PC_{61}BM$ composite we also recorded a spectrum of the electroactive component without the PS host matrix. Figure 17(a) shows the IRAV spectrum of a MEH-PPV/$PC_{61}BM$ compound (right axis scale) with equal weight ratios in comparison to the PS/MEH-PPV/$PC_{61}BM$ mixture (left axis scale). All main spectral features of these two compounds are very similar, only the weight distribution of the IRAV bands is slightly different. The spectrum of the compound without PS is enhanced approximately five times. Figure 17(b) shows the low energy part of the spectra.

IV. DISCUSSION

A. PE composites

In the PE:MEH-PPV:$PC_{61}BCR=100:1:2$ highly diluted gel no influence on the electronic structure of MEH-PPV due to the fullerene is detected. Luminescence is not quenched and no photoexcited charged states can be detected by steady state PIA. The dominant photoexcitation in the PE/MEH-PPV and PE/MEH-PPV/$PC_{61}BCR$ system, a triplet peak at 1.41 eV, is identical with results found for pristine MEH-PPV, which is manifested by intensity dependence and lifetime studies. In the free standing films we observe strong clustering of C_{60}. Film quality can be slightly improved by exchanging C_{60} with the better soluble $PC_{61}BCR$. The small amount of solvent that is purged from the gel in the early stage of forming a free standing film, is deep violet colored in the case of C_{60} and brown colored for the $PC_{61}BCR$ composite. From gel processing it is well known, that conjugated

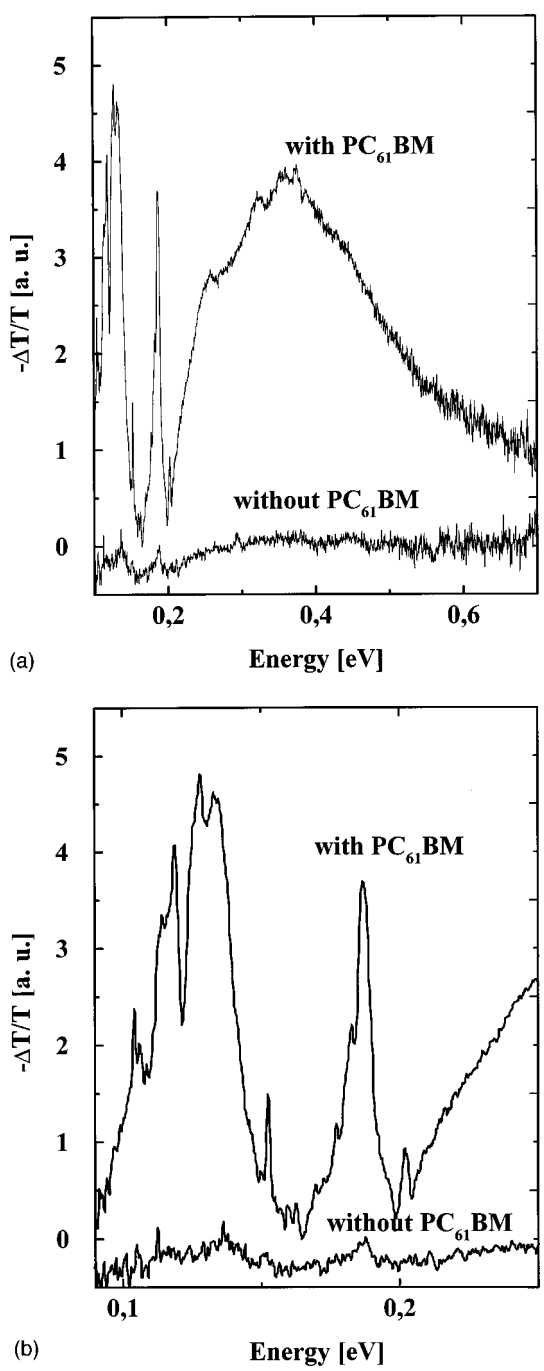

FIG. 16. Photoinduced IRAV spectrum of the PS/MEH-PPV/$PC_{61}BM$ composite and of the compound without $PC_{61}BM$ over the full region (a) and more detailed in the low energy region (b). Addition of $PC_{61}BM$ enhances IRAV features by more than ten times.

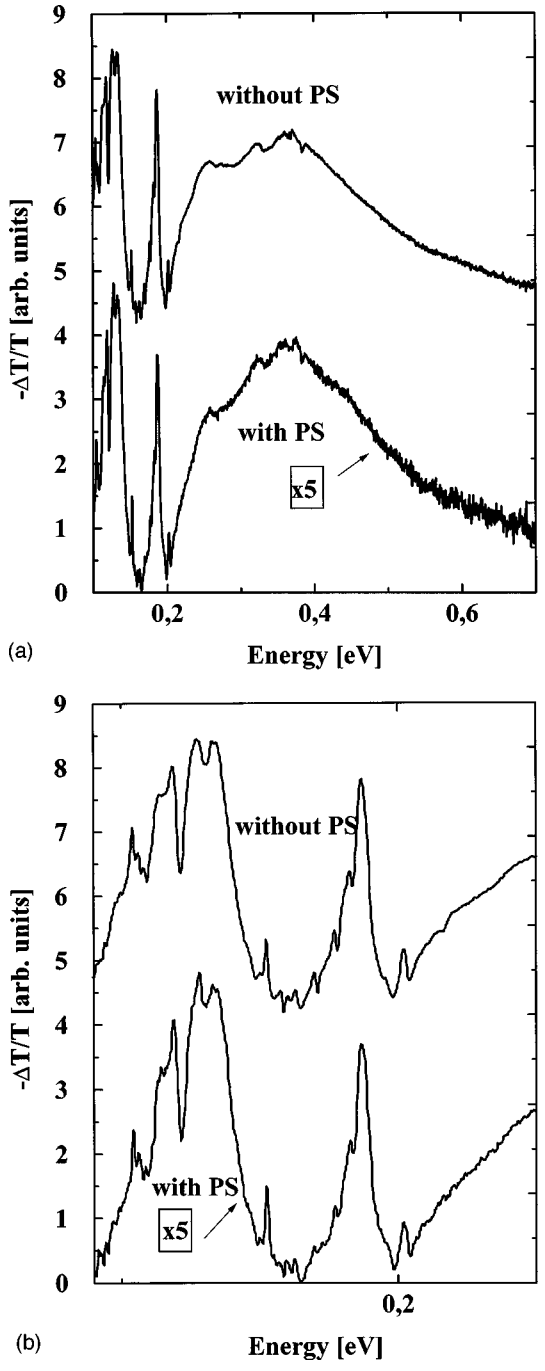

FIG. 17. Photoinduced IRAV spectrum of the PS/MEH-PPV/$PC_{61}BM$ composite (multiplied by a factor of 5) and of the compound without PS over the full region (a) and more detailed in the low energy region (b). Addition of PS lowers IRAV features by approximately six times.

polymers with a high molar mass form an interpenetrating network with PE.[19,30] This technique improves the miscibility even for less compatible polymers. For small molecules like fullerenes the formation of an interpenetrating network is not possible. Therefore, we conclude that the morphology of our PE composites can be compared to an interpenetrating network formed between PE and MEH-PPV with clusters of fullerenes in the spacings. The dimensionless interaction parameter for PE ($\delta \approx 9.6$) and C_{60} ($\delta \approx 8.1$), calculated by Flory–Huggins (F–H) theory for polymer mixtures after Hoy's table[31] gives $\chi_{12} \approx 0.38$, a value indicating the low compatibility. Furthermore, CP-MAS NMR studies on the compounds estimate the average distance between PE and C_{60} molecules larger than 1.5 nm.[32] In the highly diluted PE/MEH-PPV/C_{60} gel, the absence of any observable effect of fullerene on the photophysics of MEH-PPV in our studies is interpreted as a morphological effect of phase segregation. The same results are seen in PE/MEH-PPV/$PC_{61}BCR$ gels. However, we want to stress that these findings are only valid for highly diluted PE gels. Studies on higher concentrated

gels have been impossible due to deteriorating film quality. From all these findings we conclude, that PE gels are not suitable as matrix for fullerenes.

B. Diluted PS composites

Comparison of the F–H interaction parameter of PS ($\delta \approx 9.0$) with C_{60} gives an interaction parameter $\chi_{12} \approx 0.13$. The lower value indicates the higher compatibility of PS to C_{60} compared to PE. This assumption is manifested by the high optical quality of the films, where no fullerene aggregates can be detected with the unaided eye. Due to this more homogeneous distribution of the fullerenes we can expect higher statistical probability for MEH-PPV–C_{60} contacts in the PS matrix.

In all composites with PS as matrix we find strong luminescence quenching of the conjugated polymer upon adding C_{60}, in contrast to the results for composites using PE as matrix. Higher concentrations of C_{60} result in stronger luminescence quenching as it is known MEH-PPV/C_{60} samples. The PIA features of the reference systems, PS/MEH-PPV and PS/C_{60}, are identified as the triplet photoexcited states of the pure components, which is manifested by lifetime and intensity dependencies. We therefore conclude, that PS fulfills all conditions of an ideal host matrix. At low concentrations it forms homogeneous composites with MEH-PPV as well as C_{60} but does not directly influence the electro-optical properties of the embedded guest components.

To investigate the influence of C_{60} on the photoexcited states of PS/MEH-PPV, we studied three differently concentrated PS/MEH-PPV/C_{60} composites. While the concentration of MEH-PPV in PS is always kept at 2 wt %, the C_{60} concentrations are varied from 2 to 6 and 10 wt %. These systems are referred to as low, intermediate and high C_{60} samples.

For all PS/MEH-PPV/C_{60} composites we find photoexcited states dominated by triplet excitations. This is found by intensity dependence (Fig. 10) and lifetime studies for the broad 1.51 eV peak of the low C_{60} sample as well as for the 1.63 eV peaks of the intermediate and high C_{60} samples (Fig. 9). However, the nature of the triplets in the three samples is different.

Comparison of the lifetime and the intensity dependence of the 1.63 eV peak in the PS/C_{60} reference system with the 1.63 eV photoexcitation in the high C_{60} sample leads to the conclusion, that the dominant photoexcitation in the PS/MEH-PPV/high C_{60} system is the C_{60} triplet peak. The change of position and spectral shape of the low and intermediate C_{60} photoexcitations in comparison to the reference systems do not allow straightforward identification. Convolution studies show, that the spectrum of the intermediate C_{60} sample can be reconstructed by linear addition of the reference spectra PS/C_{60} and PS/MEH-PPV (blueshifted by 0.02 eV). This strongly implies, that the photoexcitation spectrum of the PS/MEH-PPV/intermediate C_{60} composite is dominated by the superposition of the 1.63 eV C_{60} triplet peak and by the MEH-PPV triplet peak at 1.43 eV. PIA data at two different pump energies [488 and 354 nm (Fig. 11)] clearly favors the model with two superposed peaks. Absorption correction of the UV pumped spectrum via Eq. (2) shows, that the relative intensities of the two triplet peaks are identical for both pump energies.

The spectrum of the low C_{60} sample, a broad peak located at 1.51 eV, cannot be constructed by superposition of the reference spectra. Studies at five different energetic positions of this PIA band (Fig. 10) reveal that the low energy side (MEH-PPV side) is dominated by bimolecular relaxation behavior, while the high energy side (C_{60} side) is a superposition of bimolecular as well as monomolecular behavior. However, from these data alone we cannot conclude whether this peak is one broad triplet complex (or triplet pair) or rather a superposition of energy shifted MEH-PPV and C_{60} triplet peaks. Janssen *et al.*[33] showed that dilute solutions of poly(3-alkylthiophene) and C_{60} can exhibit a triplet energy transfer from the conjugated polymer to the fullerene. In our studies we do not find a sensitization of the C_{60} triplet due to MEH-PPV excitations.

LESR spectra for none of the diluted PS composites as well as the reference systems (MEH-PPV in PS or C_{60} in PS) show photoinduced radicals in detectable quantities. The quenching of photoluminescence is a clear indication of an excited state interaction between MEH-PPV/C_{60} in PS matrices even in these dilute concentrations. However, clear evidence of photoinduced electron transfer and charge separation from conjugated polymers onto C_{60} is not observed in our PIA and LESR studies on these dilute PS composites. Also, a triplet sensitization is ruled out. The dissipation of the luminescence energy is proposed to be due to nonradiative relaxations.

C. Concentrated PS composites

From percolation theory of polymer blends[34] it is well known, that physical properties of the guest molecule show an onset at volume fractions larger than some critical value. For instance, for a three dimensional network of conducting globular aggregates in an insulating matrix classical percolation theory predicts a threshold for conductivity at a volume fraction $\approx 17\%$. This is in agreement with results obtained for composites of poly(3-alkylthiophene) in polystyrene[13] and for other conducting polymer composites.[35] This threshold can be remarkedly reduced by morphology optimization of the composite with the help of interpenetrating networks[19] to values as low as 0.3%.[36] The strong quenching of luminescence reported by Morita *et al.*[37] for mixtures of conjugated polymers with different molar ratios of fullerenes clearly shows, that the percolation threshold for photoinduced electron transfer in these systems is below the theoretical prediction of 17%.

From percolation theory it is expected, that the PS systems investigated in this work should show photoinduced electron transfer if the concentration of the donor–acceptor component exceeds some threshold. However, the critical threshold concentration for the occurrence of photoinduced electron transfer in three component systems is still unknown. Therefore, we designed the concentrated PS composite, where the concentrations of the single electroactive components are clearly over 17%, the classical polymer–small particle percolation threshold.

LESR spectra of conjugated polymer/fullerene mixtures (Figs. 12–15) unambiguously prove the occurrence of photoinduced electron transfer in the concentrated PS composites. After correction for metastable, trapped radicals, the LESR spectrum of the concentrated PS/MEH-PPV/C_{60} sample (Fig. 12) clearly shows two photoinduced radicals. Saturation analysis[28] proves, that these radicals belong to different species. According to the literature[21] these excitations are identified as a polaron on the polymer chain and a C_{60}^{-} anion. Figure 14 shows the response of the concentrated PS sample when C_{60} is exchanged by $PC_{61}BM$. Again, two photogenerated radicals are observed, at exactly the same g values as before with C_{60}. Only the intensity of the signals for the $PC_{61}BM$ sample increases considerably, indicating that electron transfer is happening with higher efficiencies. This is in accordance with earlier findings for photovoltaic devices[38] where $PC_{61}BM$ is better mixing into a polymer matrix. All these findings for electron transfer are confirmed by the enhancement of photoinduced IRAV bands upon increasing the concentration of $PC_{61}BM$ seen in Figs. 16 and 17.

V. SUMMARY

Spectroscopic studies of MEH-PPV–fullerene blends embedded into conventional polymer matrices show unusual photoexcitation features compared to pure MEH-PPV–fullerene blends. Depending on the choice of the host material and on the concentration of the photoactive guest components the nature of the photoexcited species is changed. In composites with PS as matrix we find strong luminescence quenching of the conjugated polymer upon adding small amounts of C_{60} (<1 wt %), in contrast to a system using PE as matrix. Furthermore, in diluted PE gels we do not find any signs of interaction between the fullerene–conjugated polymer components. Spectroscopic studies on PE gels with higher concentrations of the electroactive components are limited by the poor optical quality of these compounds. Dominant photoexcitations in PS systems with diluted electroactive components are triplet states, but not electron transfer. Only in PS composites with high loading of both, MEH-PPV and fullerenes, photoinduced electron transfer occurs. Thus the choice of the host material and the concentration of the electroactive guest materials are the critical parameters controlling the interfacial contacts of these composites and the resulting photophysics.

ACKNOWLEDGMENTS

We thank F. Wudl and A. J. Heeger from the IPOS, UCSB for support with $PC_{61}BCR$ and MEH-PPV as well as for support for a sabbatical stay for C.B. Parts of the research were founded by a stipendium from the Austrian BMWW. Work at UCSB was supported by the National Science Foundation under Grant OMR9300366. V.D. thanks FWF for financial support by a Lise Meitner fellowship under Grant M00419-PHY. Work was supported by FWF under Project No. P-R680-CHE.

[1] T. Skotheim, *Handbook of Conducting Polymers* (Dekker, New York, 1986).
[2] J.-L. Bredas and R. R. Chance, *Conjugated Polymeric Materials\ Opportunities in Electronics, Optoelectronics and Molecular Electronics* (Kluwer Academic, Dodrecht, 1990).
[3] W. R. Salaneck, D. T. Clark, and E. J. Samuelsen, *Science and Application of Conducting Polymers* (Hilger, Bristol, 1991) W. R. Salaneck, D. T. Clark, and E. J. Samuelsen, *Science and Application of Conducting Polymers* (Hilger, Bristol, 1991).
[4] H. S. Nalwa, *Handbook of Organic Conductive Molecules and Polymers* (Wiley, New York, 1997).
[5] L. S. Roman, M. R. Andersson, T. Yohannes, and O. Inganäs, Adv. Mater. **9**, 1164 (1997).
[6] P. M. Allemand, A. Koch, F. Wudl, Y. Rubin, F. Diederich, M. M. Alvarez, S. J. Anz, and R. L. Whetten, J. Am. Chem. Soc. **113**, 1050 (1991).
[7] N. S. Sariciftci, L. Smilowitz, A. J. Heeger, and F. Wudl, Science **258**, 1474 (1992).
[8] L. Smilowitz, N. S. Sariciftci, R. Wu, C. Gettinger, A. J. Heeger, and F. Wudl, Phys. Rev. B **47**, 13835 (1993).
[9] B. Kraabel, J. C. Hummelen, D. Vacar, D. Moses, N. S. Sariciftci, A. J. Heeger, and F. Wudl, J. Chem. Phys. **104**, 4267 (1996).
[10] R. A. J. Janssen, N. S. Sariciftci, and A. J. Heeger, J. Chem. Phys. **100**, 8641 (1994).
[11] R. A. Marcus, J. Chem. Phys. **24**, 966 (1956).
[12] R. A. Marcus, Rev. Mod. Phys. **65**, 599 (1993).
[13] S. Hotta, S. D. D. V. Rughooputh, and A. J. Heeger, Synth. Met. **22**, 79 (1987).
[14] J. S. Uhm and H.-W. Schmidt, Polym. Prep. (Am. Chem. Soc. Div. Polym. Chem.) **34**, 725 (1993).
[15] J. Moulton and P. Smith, J. Polym. Sci., Part B: Polym. Phys. **30**, 871 (1992).
[16] T. Hagler, K. Pakbaz, and A. J. Heeger, Phys. Rev. B **49**, 10968 (1994).
[17] J. C. Hummelen, B. W. Knight, F. Lepec, and F. Wudl, J. Org. Chem. **60**, 532 (1995).
[18] F. Wudl, P.-M. Allemand, G. Srdanov, Z. Ni, and D. McBRanch, in *Materials for Non-linear Optics: Chemical Perspectives*, edited by S. R. Mader, J. E. Sohn, and G. D. Stucky (The American Chemical Society, Washington, D.C., 1991), p. 683.
[19] A. Fizazi, J. Moulton, K. Pakbaz, S. D. D. V. Rughooputh, P. Smith, and A. J. Heeger, Phys. Rev. Lett. **64**, 2180 (1990).
[20] P. Smith and P. Lemstra, J. Mater. Sci. **15**, 505 (1980).
[21] X. Wei, Z. V. Vardeny, N. S. Sariciftci, and A. J. Heeger, Phys. Rev. B **53**, 2187 (1996).
[22] L. Smilowitz and A. J. Heeger, Synth. Met. **48**, 193 (1992).
[23] N. S. Sariciftci, L. Smilowitz, A. J. Heeger, and F. Wudl, Synth. Met. **59**, 333 (1993).
[24] B. Hu, Z. Yang and F. E. Karasz, J. Appl. Phys. **76**, 2419 (1994).
[25] C. Zhang, H. von Seegern, K. Pakbaz, B. Kraabel, H. W. Schmidt, and A. J. Heeger, Synth. Met. **62**, 35 (1994).
[26] D. B. Romero, M. Schaer, M. Leclerc, D. Ades, A. Siove, and L. Zuppiroli, Synth. Met. **80**, 271 (1996).
[27] X. Wei and Z. V. Vardeny, Synth. Met. **49–50**, 549 (1992).
[28] V. Dyakonov *et al.* (unpublished).
[29] K. F. Voss, C. M. Foster, L. Smilowitz, D. Mihailovic, S. Askari, G. Srdanov, Z. Ni, S. Shi, A. J. Heeger, and F. Wudl, Phys. Rev. B **43**, 5109 (1991).
[30] T. W. Hagler, K. Pakbaz, J. Moulton, F. Wudl, P. Smith, and A. J. Heeger, Polym. Commun. **32**, 339 (1991).
[31] K. L. Hoy, J. Paint Technol. **42**, 76 (1970).
[32] S. Williams (private communication).
[33] R. A. J. Janssen, N. S. Sariciftci, and A. J. Heeger, J. Chem. Phys. **100**, 8641 (1994).
[34] Aharony and D. Stauffer, *Introduction to Percolation Theory*, 2nd. ed. (Taylor & Francis, 1993).
[35] Aldissi, Synth. Met. **13**, 87 (1986).
[36] A. J. Heeger, Trends Polym. Sci. **3**, 39 (1995).
[37] S. Morita, A. A. Zakhidov, and K. Yoshino, Solid State Commun. **82**, 249 (1992).
[38] G. Yu, J. Gao, J. C. Hummelen, F. Wudl, and A. J. Heeger, Science **270**, 1789 (1995).